arXiv:cond-mat/0609166v2 [cond-mat.soft] 8 Jan 2007

Bending Moduli of Charged Membranes Immersed in Polyelectrolyte Solutions

Adi Shafir*and David Andelman†
School of Physics and Astronomy
Raymond and Beverly Sackler Faculty of Exact Sciences
Tel Aviv University, Ramat Aviv, Tel Aviv 69978, Israel

Received 1st September 2006, corrections 28th December
DOI: 10.1039/

We study the contribution of polyelectrolytes in solution to the bending moduli of charged membranes. Using the Helfrich free energy, and within the mean-field theory, we calculate the dependence of the bending moduli on the electrostatics and short-range interactions between the membrane and the polyelectrolyte chains. The most significant effect is seen for strong short-range interactions and low amounts of added salt where a substantial increase in the bending moduli of order $1\,k_BT$ is obtained. From short-range repulsive membranes, the polyelectrolyte contribution to the bending moduli is small, of order $0.1\,k_BT$ up to at most $1\,k_BT$. For weak short-range attraction, the increase in membrane rigidity is smaller and of less significance. It may even become negative for large enough amounts of added salt. Our numerical results are obtained by solving the adsorption problem in spherical and cylindrical geometries. In some cases the bending moduli are shown to follow simple scaling laws.

1 Introduction

The study of interactions between charged and flexible membranes and polyelectrolytes (PEs) in solution has generated a lot of interest in recent years, partly motivated by the importance of such interactions in biology. Understanding the interaction between charged macromolecules such as DNA, RNA and various proteins and biological cell membranes (modeled as charged and flexible interfaces) sheds light on many important cellular processes. Besides its biological significance, the adsorption of PEs onto charged membranes raises interesting questions about the interplay between short-range and electrostatic (long range) interactions in these multi-component charged systems. Recent works include numerical and analytical calculations [1, 2, 3, 4, 5, 6, 7, 8, 9, 10, 11] and scaling arguments [1, 4, 5, 12, 13].

In our previous work [14], three regimes have been found for polyelectrolyte adsorption. (i) When the *short-range interaction* between the membrane and the PE chains is repulsive, the surface charge is low and the ionic strength of the solution is high, the polymers deplete from the charged membrane. (ii) For higher surface charges, or lower ionic strength, the polyelectrolytes adsorb on the charged membrane and screen the surface charges. (iii) When the short-range interactions between the membrane and the PE chains are attractive, the PE chains adsorb on the membrane, and the adsorbed layer carries a higher charge than that of the bare membrane. In this situation the polyelectrolytes over compensate the bare surface — a phenomenon of practical importance in the build-up of multilayers of alternating cation and

*E-mail:shafira@post.tau.ac.il
†E-mail:andelman@post.tau.ac.il

anion polyelectrolytes [15].

The flexibility of fluid surfaces and membranes has been studied in various cases, and it depends on the lipid composition, tail length and molecular tilt. In the case of charged and flexible membranes immersed in a pure ionic solution (no macromolecules) [16, 17, 18, 19, 20, 21, 22, 23, 24, 25, 26, 27], the electrostatic contribution was found to increase the membrane rigidity, and the addition of salt to decrease it. In a different set of studies, the adsorption of neutral polymers on membranes has been investigated theoretically [28, 29, 30, 31, 32, 33, 34] and in experiments [35, 36, 37, 38]. It was found that the addition of polymers reduces the membrane rigidity. In all those cases, the contribution of the solution to the bending rigidity was found to be of order $0.1-1\,k_BT$, which is low in comparison to the intrinsic monolayer bending rigidity of approximately $10\,k_BT$. We note that in special cases, by adding a co-surfactant (alcohol), the membrane bending rigidity can be brought down to values of roughly $1\,k_BT$ [39].

In the present work, we study the combined system of charged chains interacting with oppositely charged and flexible membranes. Our study is similar in spirit to that done for DNA-lipid systems [40, 41], where the DNA was modeled as rigid and charged rod. The main difference is that our charged macromolecules are flexible. The above mentioned three regimes dictate a different contribution to the membrane rigidity and stability. For short-range repulsive membranes, the membrane rigidifies due to its charges while its rigidity decreases with the increase of the polyelectrolyte charge. For weak short-range interactions, the contribution to the membrane rigidity decreases and may become slightly negative, while for strong short-range attraction the membrane becomes rigid again. In most cases, the magnitude of the contribution to the bending rigidity is of the same order of magnitude as that of neutral polymers or pure salt solutions, namely $0.1\,k_BT$ up to $1\,k_BT$. However, we show in this paper that for strong enough short-range attraction a more significant contribution, of order k_BT or higher can be obtained.

2 Mean Field Equations

2.1 Free-Energy Formulation

Consider a bulk aqueous solution containing polyelectrolyte (PE) chains, along with their counter ions and added salt. A curved and charged membrane is placed at the origin $|\mathbf{r}| = 0$. In order to extract the membrane elastic moduli, we take the membrane shape to be either spherical or cylindrical with radius R . The free energy for the combined system has been formulated before [1], and can be written as a sum of four contributions $F_{\rm tot} = F_{\rm pol} + F_{\rm ions} + F_{\rm el} + F_{\rm int}$.
The polymer free energy, $F_{\rm pol}$, is:

$$F_{\rm pol} = \int_V {\rm d}\mathbf{r}\left[\frac{a^2}{6}\left|\nabla\phi\right|^2 + \Sigma\left(\phi\right) - \Sigma\left(\phi_b\right) + \mu\left(\phi^2-\phi_b^2\right)\right], \quad (1)$$

where a is the monomer size, ϕ_b^2 is the monomer bulk concentration, ϕ^2 is the local monomer concentration. The free energy is given in terms of k_BT, and the integration is carried out over the entire volume outside the sphere/cylinder, $|\mathbf{r}| > R$. The first term in Eq. (1) accounts for the chain elasticity. The second and third terms account for the excluded volume interactions in the solution and in the bulk, respectively:

$$\Sigma\left(\phi\right)a^3 = \left(1-a^3\phi^2\right)\log\left(1-a^3\phi^2\right) - \frac{1}{2}\left(v-a^3\right)\left(1-a^3\phi^2\right)\phi^2 \quad (2)$$

$$\mu = \log\left(1-a^3\phi_b^2\right) + \frac{1}{2}\left(va^{-3}+1\right) - \left(v-a^3\right)\phi_b^2 \quad (3)$$

where v is the excluded volume coefficient. For $\phi^2 \ll a^{-3}$ the above expression can be expanded to the well known $\frac{1}{2}v\left(\phi^2-\phi_b^2\right)^2$, which is commonly used for the excluded volume interaction. The small ion contribution to the entropy is:

$$F_{\rm ions} = \sum_{i=\pm}\int_V {\rm d}\mathbf{r}\left[c_i\log\frac{c_i(x)}{c_b^i} - c_i(x) + c_b^i\right] \quad (4)$$

where $c_\pm$ and $c_b^\pm$ are the local and bulk concentrations of the $\pm$ small ions, respectively. The third contribution to the free energy, the electrostatic free-energy, is:

$$F_{\rm el} = \int_V {\rm d}\mathbf{r}\left(c_+ - c_- + f\phi^2\right)\zeta - \frac{1}{8\pi l_B}\int_V {\rm d}\mathbf{r}\,|\nabla\zeta|^2 + \int_{|\mathbf{r}|=R} {\rm d}\mathbf{A}\sigma\zeta \quad (5)$$

where $\zeta \equiv e\psi/k_BT$ is the renormalized electrostatic potential, f is the fraction of charged monomers and $l_B \equiv e^2/\varepsilon k_BT$ is the Bjerrum length. The first integral accounts for the interactions between the positive ions, negative small ions and the monomer charges with the electrostatic potential. The second integral accounts for the self-energy of the electrostatic field and the third to the interaction between the surface charge and the electrostatic potential. Note that the third integral is taken only over the charged body surface, $|\mathbf{r}| = R$.

The last part of the free energy is the short-range interaction of the PE chains with the membrane:

$$F_{\rm int} = -\frac{a^2}{6d}\int_{|\mathbf{r}|=R} {\rm d}\mathbf{A}\,\phi_s^2 \quad (6)$$

where $\phi_s \equiv \phi\left(|\mathbf{r}| = R\right)$ is the monomer concentration on the surface. This term stands for a general short-range interaction, where the interaction strength is determined by the phenomenological constant d^{-1}, which has dimensions of inverse length.

Minimization of the total free energy $F_{\rm tot} = F_{\rm pol} + F_{\rm ions} + F_{\rm el} + F_{\rm int}$ yields the following mean-field equations, expressed in terms of a dimensionless variable $\eta \equiv \phi/\phi_b$:

$$\nabla^2\zeta = \lambda_D^{-2}\sinh\zeta + k_m^2\left(\mathrm{e}^{\zeta} - \eta^2\right) - 4\pi l_B\sigma\delta\left(|\mathbf{r}| - R\right) \quad (7)$$

$$\frac{a^2}{6}\nabla^2\eta = \Lambda\left(\eta\right)\eta - f\zeta\eta - \frac{a^2}{6d}\delta\left(|\mathbf{r}| - R\right)\eta \quad (8)$$

where $\lambda_D = \left(8\pi l_B c_{\rm salt}\right)^{-1/2}$ is the Debye-Hückel length scale for the screening of the electrostatic potential in the presence of added salt and $k_m^{-1} = \left(4\pi l_B\phi_b^2 f\right)^{-1/2}$ is the corresponding length for the potential decay due to counterions. Note that the actual decay of the electrostatic potential is determined by a combination of salt, counterions, and polymer screening effects. The excluded volume interaction is taken into account using the function:

$$\Lambda\left(\eta\right) = \log(1-\phi_b^2a^3) - \log(1-\phi_b^2a^3\eta^2) + \left(v - a^3\right)\phi_b^2\left(\eta^2 - 1\right) \quad (9)$$

which represents the full excluded volume interaction.

The solution of Eqs. (7) and (8) requires four boundary conditions. Two of the boundary conditions are taken far from the membrane, where the monomer concentration and electrostatic potential retrieve their bulk values $\eta\left(|\mathbf{r}| \to \infty\right) \to 1$ and $\zeta\left(|\mathbf{r}| \to \infty\right) \to 0$. The other two boundary conditions account for the interaction with the charged membrane, and can be obtained by integrating Eqs (7) and (8) from $|\mathbf{r}| = R$ to a small distance from the membrane, yielding:

$$\hat{\mathbf{n}}\cdot\nabla\zeta|_{|\mathbf{r}|=R} = -4\pi l_B\sigma \quad (10)$$

$$\hat{\mathbf{n}}\cdot\nabla\eta|_{|\mathbf{r}|=R} = -d^{-1}\eta_s \quad (11)$$

Equation (10) is the usual electrostatic boundary condition for a given surface charge density, while Eq. (11) is the Cahn - de Gennes boundary condition [42], which is often used for calculating polymer profiles [30, 31, 29].

For large R, the total free-energy can be expanded around its flat surface value in the following way [44]:

$$F_{\rm tot} = \int_{|\mathbf{r}|=R} {\rm d}\mathbf{A}\left[f_0 + \frac{1}{2}\delta\kappa\left(c_1 + c_2 - \frac{2}{R_0}\right)^2 + \delta\kappa_G c_1 c_2\right] \quad (12)$$

where $F_{\rm tot}$ is the total free energy (in units of k_BT), f_0 is the free energy per unit area of a solution in contact with a planar surface ($R \to \infty$) that has the same system parameters,

and c_1, c_2 are the radii of curvature for the membrane. For spherical surfaces the radii of curvature are $c_1 = c_2 = 1/R$, while for a cylindrical surface $c_1 = 1/R$, $c_2 = 0$. The parameters $\delta\kappa$ and $\delta\kappa_G$ are the contributions of the PE (and salt) solution to the mean and Gaussian curvature moduli of the membrane, respectively, in units of k_BT. Namely, $\kappa = \kappa^0 + \delta\kappa$ and $\kappa_G = \kappa_G^0 + \delta\kappa_G$ include the intrinsic values as well as the contributions coming from the solution. Throughout this paper we will consider only the changes in the elastic moduli κ, κ_G with respect to their bare values. An increase in the mean curvature modulus $\delta\kappa$ increases the membrane rigidity, while an increase in the Gaussian modulus $\delta\kappa_G$ makes saddle points on the membrane more favorable.

The parameter R_0 is the radius of spontaneous curvature for the membrane, which is dependent on the exact chemical composition of the membrane. For a positive R_0, the membrane bends towards the external solution, while for negative R_0 it bends away from the solution. In the case of a bilayer membrane, where the same solution is in contact with both leaflets of the membrane, the spontaneous curvature vanishes due to symmetry. In this paper, we do not calculate the spontaneous curvature but rather focus on the changes to the bending moduli $\delta\kappa$ and $\delta\kappa_G$.

2.2 Numerical Procedure

Equations (7)-(11) are solved numerically for the cases of a charged sphere and a charged cylinder. The numerical procedure follows the relaxation scheme [43], as was described in previous publications [4, 5]. For each solution, we calculate the total free energy per unit area for the cases of a spherical membrane f_S and a cylindrical membrane f_C. The contributions of the polyelectrolyte solution to the mean and Gaussian curvatures are then calculated by expanding f_C, f_S to second order in $1/R$:

$$f_S = f_0 + \frac{A_S}{R} + \frac{B_S}{R^2} \quad (13)$$

$$f_C = f_0 + \frac{A_C}{R} + \frac{B_C}{R^2} \quad (14)$$

The contributions of the solution to the curvature moduli are given by:

$$\delta\kappa = 2B_C \quad (15)$$

$$\delta\kappa_G = B_S - 4B_C. \quad (16)$$

A surface is stable under long wave bending fluctuations only when $\kappa > 0$, and against spontaneous vesiculation (topological change) when $2\kappa + \kappa_G > 0$ [24]. In the following we show that the contribution of the PE solution to the stability of a charged surface depends on the amount of added salt, and has a non-monotonic dependence on the short-range interactions between the membrane and the polyelectrolyte.

3 Results

We find large contributions, of order $1\,k_BT$, to the surface bending moduli for the case of strong short-range attractive surfaces. For weaker short-range interactions and for repulsive surfaces, the contribution is smaller, of order $0.1 - 1\,k_BT$. We discuss first the strong repulsive and strong attractive surface limits, and then turn to the intermediate case, where the contribution to the bending rigidity is less significant. We present analogies and scaling calculations to explain the different regimes.

3.1 Strong Short-Range Attractive Membranes

In previous publications [5, 6], the adsorbed amount of PEs as well as the layer width were studied in detail for short-range attractive surfaces. The adsorbed PEs charge was shown to exceed the bare surface charge significantly for strong short-range interactions, and to exceed it mildly for weak short-range interactions. The width of the adsorbed layer, on the other hand, depends on the shorter of the two adsorption length scales: (i) d, the length scale for short-range attraction from Eq. (11), and (ii) $\xi \equiv a/\sqrt{v\phi_b^2}$, the Edwards correlation length for neutral polymer adsorption. In our model, we use an almost theta solvent $0 < v\phi_b^2 \ll 1$, so we

assume that the shorter length scale is always $d \ll \xi$. The increase in short-range attractive interactions, in this case, decreases the adsorbed layer width [4, 5]. The combined charge of the PE-membrane complex is, therefore, opposite to the initial surface charge, and its magnitude may be much higher than the initial membrane charge. This charge is distributed within a layer of width d close to the surface.

Our focus in this section is on the low salt case. In Fig. 1 we show the dependence of κ and κ_G on the short-range interaction parameter d^{-1} for low salt conditions. For strong short-range attraction, namely $d < 2$Å, the calculated $\delta\kappa$ is positive and increases strongly, reaching values of several k_BT. The $\delta\kappa_G$ is negative, and shows a stronger increase with d^{-1} than the corresponding $\delta\kappa$. The contribution to the vesiculation stability $2\delta\kappa+\delta\kappa_G$ in this case can be seen to be negative for high d^{-1}, leading to destabilization of the surface. For lower (but positive) d^{-1}, the contribution to $2\delta\kappa + \delta\kappa_G$ is positive, and thus enhances the membrane stability.

These results can be explained by the following argument. When the adsorbed layer width is smaller than the electrostatic screening length, the membrane-PE complex can be viewed as a renormalized charged surface, containing both the bare surface charges and the adsorbed PE charges, in a weak ionic solution. The renormalized surface interacts with the ionic solution in the same manner as a bare membrane [16, 17, 18, 19, 20, 21, 22, 23, 24]. The strong increase in the surface charge and the lack of small ion screening (low salt) cause the surface fluctuations to be strongly unfavorable, making $\delta\kappa$ positive. This allows substantial increase in the magnitude of $\delta\kappa$, $\delta\kappa_G$, amounting to several k_BT, which is a significant contribution to the membrane curvature moduli, as can be seen in Fig. 1. We note that as the renormalized surface charge increases, the value of $\delta\kappa$ should approach the low salt limit for charged surfaces in pure ionic solutions (no PE) $\delta\kappa \to \lambda_D/(2\pi l_B) \simeq 7\, k_BT$ [24] (See Fig. 1). However, this limit is still higher than our numerical results for the PE-membrane complex.

The crossover between positive and negative values of $2\delta\kappa + \delta\kappa_G$ can also be explained by analogy to ionic solutions. There are two regimes for $2\delta\kappa+\delta\kappa_G$ in pure ionic solutions [24], depending on the surface charge. For weakly charged surfaces $c_{\rm salt} \gg l_B\,|\sigma|^2$ (or $\lambda_D \ll \lambda_{\rm GC}$ where $\lambda_{\rm GC} \equiv (2\pi l_B\,|\sigma|)^{-1}$ is the Gouy-Chapman length), $\delta\kappa$ as well as $2\delta\kappa + \delta\kappa_G$ are positive [18, 20], while for highly charged surfaces $c_{\rm salt} \ll l_B\,|\sigma|^2$ we get $\delta\kappa > 0$ and $2\delta\kappa + \delta\kappa_G < 0$ [21, 22]. In our case of polyelectrolyte solutions, for low enough attractive short-range interactions the renormalized surface charge is low, and $2\delta\kappa + \delta\kappa_G > 0$. For stronger short-range interactions, the renormalized surface charge increases and $2\delta\kappa+\delta\kappa_G < 0$. The results in Fig. 1 were presented in the low added salt case, $d \ll \lambda_D$. When more salt is added into the solution the electrostatic interactions between the polymers become weaker. In case of a high amount of added salt, $d \gg \lambda_D$, the charges of the adsorbed polymers are screened over smaller length scales than the adsorbed layer width, and the analogy to a renormalized charged surface breaks down. We further discuss this case in Sec. 3.3.

3.2 Short-Range Repulsive Membranes

Without the PE adsorption, the charges on the membrane increase the membrane rigidity, κ, due to the long-range repulsion between them. For strongly repulsive surfaces, the adsorption of PE chains to the membrane screens its surface charges and causes κ to decrease. Note that the PE charges do not fully compensate the membrane bare charges like they do in the strongly attractive regime, leading to the difference in the corresponding system behaviors.

There are two regimes for the case of short-range repulsive membranes: (i) the low-salt regime where the surface charges are mainly balanced by the adsorbed monomer charges, and (ii) the high-salt regime where the salt ions screen the surface charges and the monomers deplete. The bending moduli in the latter regime are similar to those of a strong ionic solution with no added PE, as were discussed in detail in other papers [16, 17, 18, 20, 24].

In Ref. [4] we addressed the PE adsorption

close to a *flat* charged surface and showed that the screening length of the electrostatic potential depends strongly on the amount of added salt. For low salt conditions, the surface charges are screened mainly by the adsorbed monomer charges. In this case the free-energy per unit area scales like $f_{\rm ads} \sim |\sigma|^{5/3} f^{-1/3} a^{2/3} l_B^{2/3}$ and the screening length scales like $D \sim a^{2/3}/(f l_B |\sigma|)^{1/3}$ [4]. For high amounts of added salt, the screening is mainly done by small ions and the PE chains deplete. The transition from depletion to adsorption regimes occurs when the screening length due to monomer adsorption becomes similar to the one for small ion adsorption, i.e., when $\lambda_D \sim D$.

The flat surface results can now be easily extended to curved surfaces. In the low-salt regime, monomers are adsorbed to the membrane, and the length scale for the adsorption is D. We expect the free energy of the curved membrane (per unit area) to scale like $f_{\rm tot} = f_{\rm ads} h\,(D/R)$. Expanding $f_{\rm tot}$ to second order in R^{-1} and comparing to Eq. (12) shows that both curvature moduli scale like:

$$\delta\kappa,\, \delta\kappa_G \sim f_{\rm ads} D^2 \sim \frac{|\sigma|\, a^2}{f}, \qquad (17)$$

which is of order $0.1 - 1\, k_B T$ for physiological range of system parameters.

In Fig. 2 we present the values of $\delta\kappa$ and $\delta\kappa_G$ as a function of the surface charge $|\sigma|$, in the case of strongly repulsive membranes $d^{-1} = -20\,\text{Å}^{-1}$ and monomer size of $a = 10\,\text{Å}$. For low amounts of added salt we find a scaling relation $\delta\kappa,\, \delta\kappa_G \sim |\sigma|^{\beta}$ with $\beta \simeq 1.2$. Note that the numerically calculated exponent $\beta \simeq 1.2$ is slightly larger than $\beta = 1$ derived in Eq. (17). This discrepancy seems to occurs because the high monomer size used here makes the full excluded volume interaction substantial. For comparison, we plot the corresponding $\delta\kappa$, $\delta\kappa_G$ for the case of a pure ionic solution, namely when no polyelectrolytes are added to the solution. In this case the magnitudes of both $\delta\kappa$, $\delta\kappa_G$ are very high. This shows that the addition of polyelectrolytes into low salt solutions can cause a strong reduction of the bending moduli, in the order of several $k_B T$ as compared with the pure salt solution. This reduction can be explained by the fact that the polyelectrolytes replace the salt ions in screening the surface charges, thus allowing greater membrane flexibility.

In the high salt regime, the membrane interacts only with the small ions, and the polymer chains are depleted. The free energy in this case is similar to that of a weakly charged surface in an ionic solution [24]. Namely, the screening length is λ_D and the free energy per unit area for the case of a flat surface is $f_{\rm dep} \sim |\sigma|^2 l_B \lambda_D$. The curvature moduli are the same as in a pure ionic solution [16, 17, 18, 20, 24], where:

$$\delta\kappa,\, \delta\kappa_G \sim f_{\rm dep} \lambda_D^2 \sim |\sigma|^2 l_B \lambda_D^3. \qquad (18)$$

Note that the depletion condition $\lambda_D < D$ implies that the bending moduli for the high salt (depletion) case are always lower than for low salt (adsorption) case, despite the depletion of the polymers. Both $\delta\kappa$ and $\delta\kappa_G$ in this case are of order $0.01 - 0.1\, k_B T$ for physiological range of system parameters, and scale like $|\sigma|^2$.

For both low and high salt regimes, the contribution to the Gaussian bending modulus $\delta\kappa_G$ is negative, resulting from the electrostatic repulsion between the membrane constituents [19]. The contribution of the PE solution to the vesiculation stability $2\delta\kappa + \delta\kappa_G$ is always positive, even for very low salt concentrations, in contrast to the pure ionic solution results [21, 22, 23]. The low-salt regime of the ionic solutions, in which the contribution to $2\delta\kappa + \delta\kappa_G$ is negative, is replaced here by the adsorption regime, in which this contribution is still positive.

3.3 Weak Short-Range Interacting Membranes

In Fig. 3 we present an enlargement of Fig. 1 for surfaces having only a weak short-range interaction with the PE in solution, $d^{-1} \sim 0$. As can be seen, the magnitudes of both $\delta\kappa$ and $\delta\kappa_G$ decrease substantially for low $|d^{-1}|$, and may become negative for high values of added salt. The decrease in the magnitude of the bending moduli can be attributed to the strong screening of the surface charges by the adsorbed PEs, which makes $\delta\kappa$ smaller. We note that the contribution to $\delta\kappa$ and $\delta\kappa_G$ is negligible in compar-

ison to the membrane intrinsic bending moduli, and probably cannot be observed experimentally. This regime is presented only in order to complete the d^{-1} dependence picture.

For low and positive d^{-1} and high amounts of added salt, we find a negative contribution to the mean curvature modulus due to the polymer adsorption $\delta\kappa < 0$, as well as in $2\delta\kappa + \delta\kappa_G$. This surprising result can be explained by analogy to the neutral polymer case. In past publications [29, 30, 31] it was shown that neutral polymer solutions have negative $\delta\kappa$, positive $\delta\kappa_G$ and negative $2\delta\kappa + \delta\kappa_G$. We find here similar results.

The analogy to neutral polymer adsorption is important and can be understood in the following way. The high amount of added salt screens both the surface and the PE charges, so their effective interaction becomes short-ranged leading the way to an almost neutral polymer behavior. The increase in $\delta\kappa_G$ derives from the effective attraction between membrane constituents, which results from their short-range attraction to the PE chains. The analogy to neutral polymers requires the screening length for the electrostatic interactions to be much smaller than the layer width $\lambda_D < d$. This is satisfied in high salt and low short-range attraction conditions. For stronger short-range interactions, the layer width decreases, and the electrostatic interactions between monomers becomes important. In this case, the analogy to neutral polymers breaks down, and $\delta\kappa$, $2\delta\kappa + \delta\kappa_G$ start to increase back. For higher d^{-1}, both $\delta\kappa$ and $2\delta\kappa + \delta\kappa_G$ become positive again, marking the crossover to the strong attraction regime described in Sec. 3.1 above. This can be seen in Fig. 3, where for high amounts of added salt, the increase in $\delta\kappa$ with d^{-1} indeed begins when $\lambda_D \simeq d$, as expected from the above analysis. It is also important to note, that the magnitude of both $\delta\kappa$ and $\delta\kappa_G$ are very small, of order $0.01\,k_BT$, and are negligible in comparison to the intrinsic bending moduli of a membrane, of order $10\,k_BT$. The decrease shown here cannot account for a decrease in membrane rigidity that was recently found for DNA adsorption [46].

4 Conclusions

In this paper we show that the interaction between charged and flexible polymers (PE) and oppositely charged and flexible membrane depends both on their electrostatic and short-range interactions. A non-monotonic dependence of the curvature moduli is obtained as function of the short-range interaction between the membrane and the PE chains. We find a significant contribution to the bending moduli, of order of several k_BT, in the case of strong short-range attraction between the PE chains and the surface. For *weak* attractive interactions, the contribution of the PE solution to the membrane curvature moduli is small (in units of k_BT), and for repulsive interactions it increases back, and may reach values of $0.1 - 1\,k_BT$.

Our work deals only with uniformly charged membranes. In biological membranes, however, the membrane is composed of a mixture of neutral and charged lipid. The lipid molecules can rearrange and can cluster around oppositely charged PE [47]. This in turn can have a strong effect on the overall membrane rigidity. Future works may offer extensions of the present one by calculating the contributions to the spontaneous radius of curvature R_0, especially in the case of asymmetrical solutions, or when the membranes are composed of asymmetric inner and outer leaflets. Other potential directions may include changes in the effective lipid headgroup size and water activity due to the presence of polyelectrolytes.

Acknowledgments: The authors wish to thank Michael Kozlov for helpful discussions. Support from the Israel Science Foundation (ISF) under grant no. 160/05 and the US-Israel Binational Foundation (BSF) under grant no. 287/02 is gratefully acknowledged.

Adi Shafir,[a] **David Andelman**[a]
[a] *School of Physics and Astronomy*
Raymond and Beverly Sackler Faculty of Exact Sciences
Tel Aviv University, Ramat Aviv, Tel Aviv 69978, Israel.

References

[1] I. Borukhov, D. Andelman, H. Orland, *Macromolecules*, 1998, **31**, 1665; *Europhys. Lett.*, 1995, **32**, 499.

[2] I. Borukhov, D. Andelman, H. Orland, *Eur. Phys. J. B*, 1998, **5**, 869.

[3] I. Borukhov, D. Andelman, H. Orland, *J. Phys. Chem. B*, 1999, **103**, 5042.

[4] A. Shafir, D. Andelman, R.R. Netz, *J. Chem. Phys.*, 2003, **119**, 2355.

[5] A. Shafir, D. Andelman, *Phys. Rev. E*, 2004, **70**, 061804.

[6] Q. Wang, *Macromolecules*, 2005, **38**, 8911.

[7] F.W. Wiegel, *J. Phys A: Math. Gen.*, 1977, **10**, 299.

[8] M. Muthukumar, *J. Chem. Phys.*, 1987, **86**, 7230.

[9] J.F. Joanny, *Eur. Phys. J. B.*, 1999, **9**, 117.

[10] R. Varoqui,*J. Phys. II (France)*, 1993, **3**, 1097.

[11] R. Varoqui, A. Johner, A. Elaissari, *J. Chem. Phys.*, 1991, **94**, 6873.

[12] O.V. Borisov, E.B. Zhulina, T.M. Birshtein, *J. Phys. II (France)*, 1994, **4**, 913.

[13] A.V. Dobrynin, A. Deshkovski, M. Rubinstein, *Macromolecules*, 2001, **34**, 3421.

[14] A. Shafir, D. Andelman, *Phys. Rev. E.*, 2006, **74**, 021803.

[15] G. Decher, J. B. Schlenoff, *Multilayer Thin Films*, Wiley-VCH, Weinheim (2002).

[16] D. Bensimon, F. David, S. Leibler, A. Pumir, *J. Phys. (France)*, 1990, **51**, 689.

[17] A. Fodgen, B. W. Ninham, *Langmuir*, 1991, **7**, 590.

[18] M. Winterhalter, W. Helfrich, *J. Phys. Chem.*, 1988, **92**, 6865.

[19] M. Winterhalter, W. Helfrich, *J. Phys. Chem.*, 1992, **96**, 327.

[20] M. Kiometzis, H. Kleinert, *Phys. Lett. A*, 1989, **140**, 520.

[21] H.N.W. Lekkerkerker, *Physica A*, 1989, **159**, 319.

[22] D. J. Mitchell, B. W. Ninham, *Langmuir*, 1989, **5**, 1121.

[23] A. Fodgen, D. J. Mitchell, B. W. Ninham, *Langmuir*, 1990, **6**, 159.

[24] D. Andelman, in *Handbook of Biological Physics: Structure and Dynamics of Membranes*, Vol. 1B, ed. R. Lipowsky and E. Sackmann, Elsevier Science B.V., Amsterdam, 1995, Chap. 12, p. 603.

[25] H. von Berlepsch, R. de Vries, *Eur. Phys. J. E*, 2000, **1**, 141.

[26] P. A. Barneveld, D. E. Hesselink, F. A. M. Leermakeers, J. Lyklema, J. M. H. M. Scheutjens, *Langmuir*, 1994, **10**, 1084.

[27] M. M. A. E. Claessens, B. F. van Oort, F. A. M. Leermakers, F. A. Hoekstra, M. A. Cohen Stuart, *Biophys. J.*, 2004, **87**, 3882.

[28] P. G. de Gennes, *J. Phys. Chem*, 1990, **94**, 8407.

[29] J. Brooks, C. Marques, M. Cates, *Europhys. Lett.*, 1991, **14**, 713; *J. Phys. II (France)*, 1991, **1**,673.

[30] F. Clement, J-F. Joanny, *J. Phys. II (France)*, 1997, **7**, 973.

[31] K.I. Skau, E.M. Blokhuis, *Eur. Phys. J. E*, 2002, **7**,13.

[32] C. Heidgarst, R. Lipowsky, *J. Phys II (France)*, 1996, **6**, 1465.

[33] W. Sung, S. Lee, *Europhys. Lett.*, 2004, **68**, 596.

[34] M. Breidenich, R. R. Netz, R. Lipowsky, *Eur. Phys. J. E*, 2001, **5**, 403.

[35] G. Bouglet, C. Ligoure, A.M. Bellocq, E. Dufourc, G. Mosser, *Phys. Rev. E.*, 1998, **57**, 834.

[36] J. Appell, C. Ligoure, G. Porte, *J. Stat. Mech.: Theory and Exp.*, 2004, P08002.

[37] G. Gompper, H. Endo, M. Mihailescu, J. Allgaier, M. Monkenbusch, D. Richter, B. Jakobs, T. Sottmann, R. Strey *Europhys. Lett.*, 2001, **56**, 683.

[38] M. Maugey, A.M. Bellocq, *Langmuir*, 2001, **17**, 6740.

[39] D. Roux, C.R. Safinya, *J. Phys. (France)*, 1988, **49**, 307.

[40] S. May, D. Harries, A. Ben-Shaul, *Biophys. J.*, 2000, **78**, 1681.

[41] D. Harries, S. May, W.M. Gelbart, A. Ben-Shaul, *Biophys J.*, 1998, **75**, 159.

[42] P.G. de Gennes, *Macromolecules*, 1981, **14**, 1637.

[43] W.H. Press, B.P. Flannery, S.A. Teukolsky, W.T. Vetterling, *Numerical Recipes in C: The Art of Scientific Computing*, Cambridge University, Cambridge, 1992, Chap. 17, p. 762.

[44] W. Helfrich, *Z. Naturaorsch.*, 1973, **28c**, 693.

[45] K.I. Skau, E.M. Blokhuis, *Macromolecules*, 2003, **36**,4637.

[46] A. Frantescu, S. Kakorin, K. Toensing, E. Neumann, *Phys. Chem. Chem. Phys.*, 2005, **7**, 4126.

[47] S. Tzlil and A. Ben-Shaul, *Biophys. J.*, 2005, **89**, 2972.

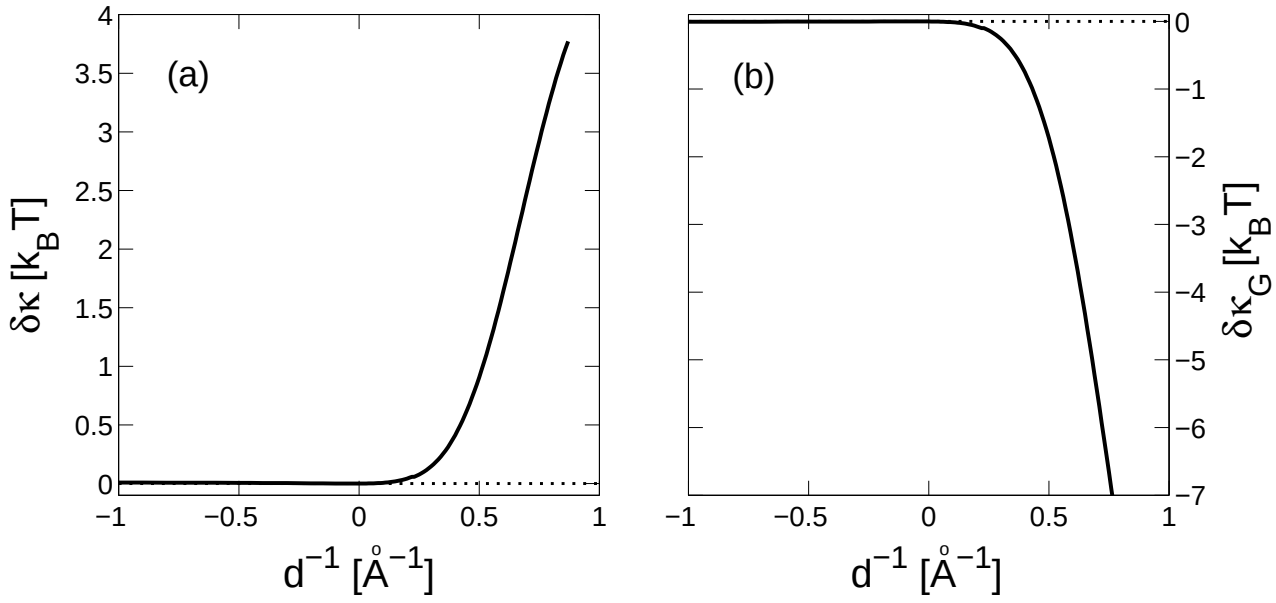


Figure 1: The d^{-1} dependence of (a) $\delta\kappa$ and (b) $\delta\kappa_G$ is presented for low added salt concentration ($c_{\rm salt} = 0.1\,{\rm mM}$). Other parameters are $|\sigma| = 0.001\,{\rm \AA}^{-2}$, $a = 5\,{\rm \AA}$, $f = 0.5$, $v = 50\,{\rm \AA}^3$, $\phi_b^2 = 10^{-8}\,{\rm \AA}^{-3}$, $T = 300\,{\rm K}$ and $\varepsilon = 80$. For large d^{-1}, we see a significant increase in the magnitude of both $\delta\kappa$ and $\delta\kappa_G$, amounting to several k_BT, which is very significant in comparison to normal membrane curvature moduli.

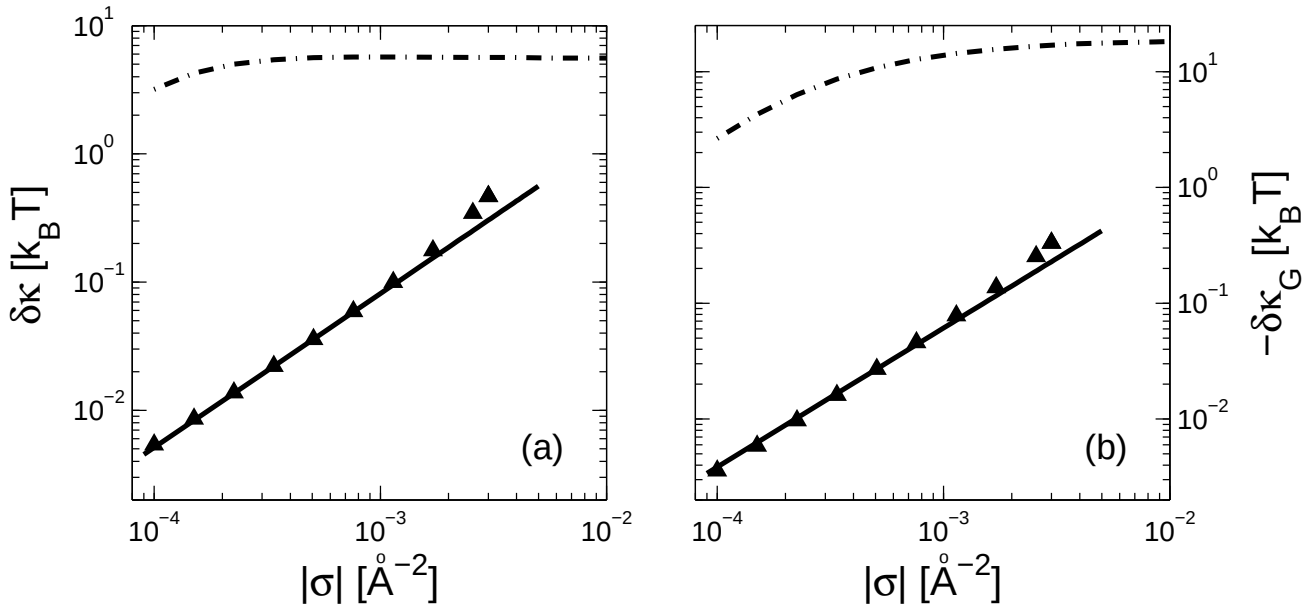


Figure 2: The dependence of $\delta\kappa$ (a) and $\delta\kappa_G$ (b) on the surface charge is presented for the case of repulsive membranes. The triangular symbols are the numerically calculated $\delta\kappa$ for $c_{\rm salt} = 0.1\,{\rm mM}$, $a = 10\,\text{Å}$, $f = 0.5$, $v = 50\,\text{Å}^3$, $\phi_b^2 = 10^{-8}\,\text{Å}^{-3}$, $T = 300\,{\rm K}$ and $\varepsilon = 80$. The solid line scales as $|\sigma|^\beta$ with $\beta \simeq 1.2$. As can be seen, for low salt concentrations the exponent of the curvature modulus, $\beta \simeq 1.2$, is close to the predicted $\beta = 1$ derived from Eq. (17). The dashed-dotted line is the numerically calculated $\delta\kappa$, $\delta\kappa_G$ for the case of an ionic solution with no polymers, with parameters $c_{\rm salt} = 0.1$ mM, $T = 300\,{\rm K}$ and $\varepsilon = 80$. The addition of polyelectrolytes can, in this case, reduce the curvature moduli significantly.

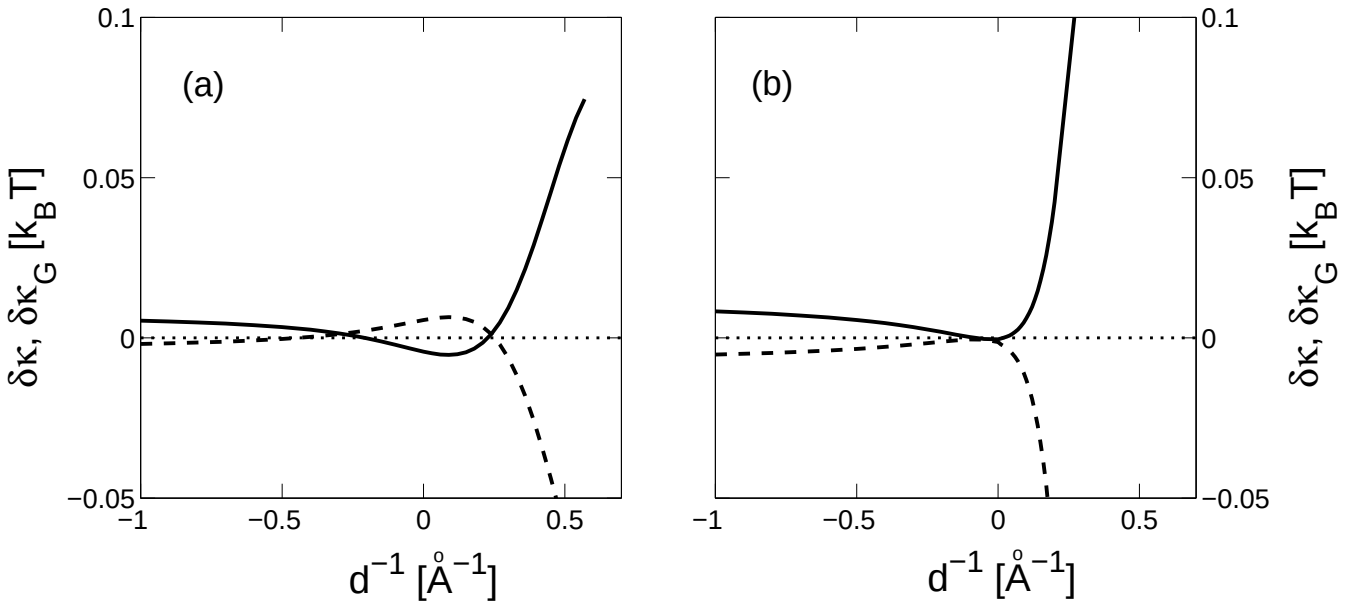


Figure 3: The d^{-1} dependence of $\delta\kappa$ and $\delta\kappa_G$ is presented for two salt concentrations: (a) $c_{\rm salt} = 0.1\,{\rm M}$ and (b) $c_{\rm salt} = 0.1\,{\rm mM}$. Other parameters are $|\sigma| = 0.001\,{\rm \AA}^{-2}$, $a = 5\,{\rm \AA}$, $f = 0.5$, $v = 50\,{\rm \AA}^3$, $\phi_b^2 = 10^{-8}\,{\rm \AA}^{-3}$, $T = 300\,{\rm K}$ and $\varepsilon = 80$. In both plots, the solid line corresponds to $\delta\kappa$ and the dashed one to $\delta\kappa_G$. Three regimes for both curvature moduli are seen. For $d^{-1} < 0$ we obtain $\delta\kappa > 0$ and $\delta\kappa_G < 0$, for $d^{-1} \sim 0$ the sign of both is inverted, and for $d^{-1} \gg 0$ both moduli return to their original sign. The magnitude of both moduli is very small for this parameter range.